IEEE Photonics Journal
An IEEE Photonics Society Publication

Open Access

Multiantenna GPS-Over-Fiber System for Attitude Determination Using Phase-Derived Range Measurement

Volume 11, Number 4, August 2019

Xiangchuan Wang
Xin Jiang
Shupeng Li
Shilong Pan, ***Senior Member, IEEE***

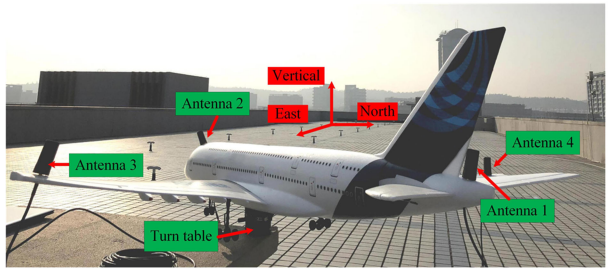

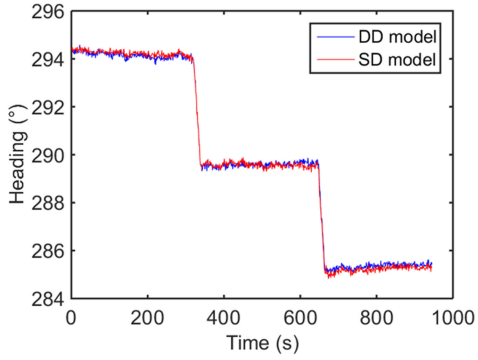

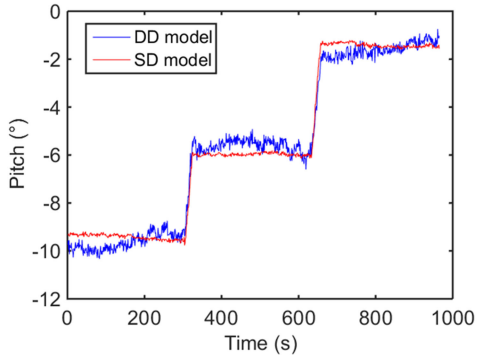

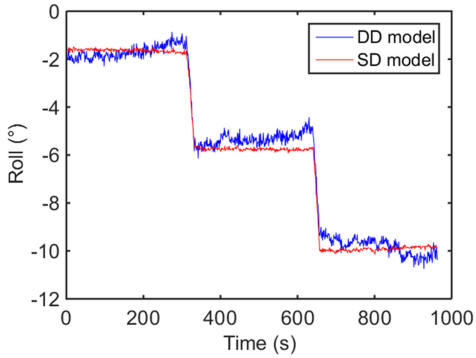

DOI: 10.1109/JPHOT.2019.2921666
1943-0655 © 2019 IEEE

Multiantenna GPS-Over-Fiber System for Attitude Determination Using Phase-Derived Range Measurement

Xiangchuan Wang, Xin Jiang, Shupeng Li, and Shilong Pan, *Senior Member, IEEE*

The Key Laboratory of Radar Imaging and Microwave Photonics, Ministry of Education, Nanjing University of Aeronautics and Astronautics, Nanjing 210016, China

DOI:10.1109/JPHOT.2019.2921666

Manuscript received May 3, 2019; revised May 30, 2019; accepted June 4, 2019. Date of publication June 7, 2019; date of current version July 4, 2019. This work was supported in part by the National Natural Science Foundation of China (61605077, 61527820), in part by Jiangsu Provincial "333" Project (BRA2018042), in part by Fundamental Research Funds for the Central Universities (NT2019011), and in part by Young Elite Scientists Sponsorship Program by CAST (2018QNRC001). Corresponding author: Shilong Pan (e-mail: pans@nuaa.edu.cn).

Abstract: A multiantenna global positioning system over fiber (GPS-over-fiber) system with real-time line bias monitoring is proposed for attitude determination of vehicles. In the proposed system, GPS signal transmission from multiple antennas to the receiver is achieved via radio-over-fiber links. A phase-derived range measurement scheme is applied to monitor the line bias variation between different optical fibers. Then the carrier phase single difference (SD) model, instead of the carrier phase double difference (DD) model, is used to improve the pitch and roll precision of the GPS-based attitude determination system. Experimental results show that the precision of the pitch and roll is improved by over three times compared with the conventional DD model while the precision of the heading is not reduced.

Index Terms: GPS over fiber, attitude determination, line bias, phase derived range.

1. Introduction

The increasing demand for navigation has led to a growing number of GPS applications in the vehicles. In addition to positioning and velocimetry, attitude determination is of critical importance for the emerging control system in vehicles for earth and space [1]–[4], including course-keeping and collision avoidance [5], [6]. Compared with the conventional inertial navigation system [7]–[9], GPS has obvious advantages in terms of maintenance-free, long-term stability and high precision. Recently, GPS has been further explored and integrated with other technologies. A low-cost but effective GPS-aided method based on the target images was proposed to measure the platform attitude angles [10]. A cooperative navigation technique which exploits GPS and relative vision-based sensing was proposed to provide accurate unmanned aerial vehicle (UAV) attitude determination [11]. Fast Alignment of the strap-down inertial navigation system was achieved based on the GPS and odometer [12]. For the multi-antenna GPS-based attitude determination system, multiple antennas are rigidly fixed to a vehicle, and then baselines are defined as vectors from auxiliary antennas to a main antenna. In the attitude determination applications, the GPS works in the relative positioning mode, and carrier phase difference technology is used to calculate the baseline with a precision

of sub-centimeter level. Precise heading and elevation angles can be therefore determined in real time [13].

Conventional GPS-based attitude determination systems consist of multiple distributed antennas and a single GPS receiver which is non-common clock scheme and electrical cables are used to connect the antennas and the receiver, which faces the following challenges in practical applications. First, complex aerospace systems require a small-size, light-weighted and anti-electromagnetic interference attitude determination device, which makes the conventional electrical-cable-connected GPS system no longer a promising solution. Second, spatial errors can be greatly eliminated by the carrier phase difference technology in the horizontal direction but its vertical resolution is unsatisfying because the distribution of satellites is uniform and symmetrical in the horizontal directions while asymmetrical in the vertical direction [14]. In practical, the DD model [11], [13], [15], [16] has been widely utilized to eliminate the spatial errors but with relative low vertical precision. The lower precision of the vertical component further deteriorates the precision of the pitch and roll angles.

For the first problem, a small-sized, light-weighted optical fiber system with low transmission loss and anti-electromagnetism interference capability could be a promising solution. Previously, a GPS-over-fiber system was constructed for aircraft attitude determination [17], [18], which applied optical fiber for the transmission of differential GPS signals. For the second problem, recent researches show that the GPS-based attitude determination system can benefit from the SD model with a clock-synchronized receiver. The multi-antenna synchronous receiver was proposed and 2 times improvement of vertical precision was achieved by the SD model through simulation analysis [19]. In theory, the measurement noise of the SD model is $1/\sqrt{2}$ times lower than that of the DD model, and the observation number of the SD model is more than that of the DD model. Therefore, the vertical accuracy of the baseline can be greatly improved by utilizing the SD model, resulting in tremendous accuracy improvement of the pitch and roll angles in the attitude determination system [16]. The SD model also has the following advantages. First, a higher success rate of integer ambiguity resolution can be realized by using the carrier phase SD model with a common clock scheme [20]. With more observations, the SD model strength is enhanced with more redundancy. Second, the carrier phase SD model can be applied to the combination of GPS and GLONASS [21]. For the same satellite, the use of between-receiver carrier phase SD model can guarantee that the ambiguity term is an integer, while the use of between-satellite carrier phase DD model is infeasible because carrier frequencies are different between GLONASS satellites.

In order to employ the ideal SD model which can strongly improve both the reliability and the precision, real-time line bias monitoring should be realized at first. Line bias reflects the different time delays of signal paths between antennas and the receiver [22]. Therefore, the line bias is an inconstant term because the time delays actually vary in time due to the environmental temperature variation and mechanical forces in practical applications. To utilize the SD model, making the antenna cables equal in length to minimize the line bias is reasonable but a hardly sufficient condition [16]. For real-time line bias monitoring, a GPS-over-fiber system with real-time line bias monitoring is proposed in which two optical fibers are utilized in one transmission link [23]. In the above system, only when the lengths of the two optical fiber changes synchronously will the measurement of the line bias delay be exact. Recently, we have proposed a GPS-based deformation monitoring system in which the line bias parameter was obtained based on the optical frequency domain reflectometer (OFDR) using a linear frequency modulated signal with large bandwidth [24].

In order to realize a small-size, light-weighted and anti-electromagnetic interference attitude determination system with a real-time line bias measurement component to improve the attitude precision, a multi-antenna GPS-over-fiber architecture based on radio-over-fiber techniques and phase-derived line bias monitoring is proposed. The line bias is related to the phase of the monitoring signal. Compared with our earlier work in ref [24], the phase-derived range measurement has a simpler structure and higher precision, which is utilized in the attitude determination application. Experiments are carried out to analyze the performance of the line bias delay monitoring and the precision of the proposed system.

2. Principle

2.1 Carrier Phase SD Model With Line Bias Compensation

The carrier phase measurement can be written as [15]:

$$\lambda\phi_i^k = \rho_i^k - I_i^k + T_i^k + c(\delta t_i - \delta t^k) + lb_i + \lambda N_i^k + e_i \tag{1}$$

where λ is the wavelength of the carrier, ϕ_i^k is the carrier phase observation, k represents the satellite's number, i denotes the antenna's number, ρ_i^k is the geometric range between the kth satellite and the ith antenna, I and T denote the ionosphere and tropospheric delay, c is the light speed in vacuum, δt denotes the clock bias, lb_i denotes the line bias delay between the antenna and the receiver, N_i^k denotes the integer ambiguity, and e_i is the observational noise.

The SD model can be obtained by making a difference of the carrier phase measurement between two antennas,

$$\lambda\Delta\phi_{ij}^k = \Delta\rho_{ij}^k + c\Delta\delta t_{ij} + \Delta lb_{ij} + \lambda\Delta N_{ij}^k + \Delta e_{ij} \tag{2}$$

where Δ is the SD operation. The distance from a satellite to an antenna is much larger than that between two antennas, so $\Delta\rho_{ij}^k$ can be approximately written as:

$$\begin{aligned}\Delta\rho_{ij}^k &\approx |\boldsymbol{b}|\cos\theta_k \\ &= \boldsymbol{s}^k\boldsymbol{b}^T\end{aligned} \tag{3}$$

where $\boldsymbol{b} = [\,b_x \quad b_y \quad b_z\,]$ is the baseline vector, $\boldsymbol{s}^k = [\,\boldsymbol{s}_x^k \quad \boldsymbol{s}_y^k \quad \boldsymbol{s}_z^k\,]$ is the normalized line of sight vector to the kth satellite, $\boldsymbol{b}^T$ is the transposed matrix of $\boldsymbol{b}$.

The receiver's clock bias is eliminated if a clock synchronous GPS receiver is used:

$$\Delta\delta t_{ij} = \delta t_i - \delta t_j = 0 \tag{4}$$

When the number of the visible satellites is n, with Eqs. (2)–(4), the SD model can be expressed as

$$\lambda\begin{bmatrix}\Delta\phi_{ij}^1\\ \Delta\phi_{ij}^2\\ \cdots\\ \Delta\phi_{ij}^n\end{bmatrix}_{n\times 1} = \begin{bmatrix}\boldsymbol{s}^1\\ \boldsymbol{s}^2\\ \cdots\\ \boldsymbol{s}^n\end{bmatrix}\boldsymbol{b}^T + \begin{bmatrix}1\\ 1\\ \cdots\\ 1\end{bmatrix}\Delta lb_{ij} + \lambda\begin{bmatrix}\Delta N_{ij}^1\\ \Delta N_{ij}^2\\ \cdots\\ \Delta N_{ij}^n\end{bmatrix}_{n\times 1} \tag{5}$$

In the processing unit at the local station, the carrier phase measurement ϕ_i^k can be directly obtained, so the vector in the left hand of Eq. (5) can be derived. The approximate positions of the antennas and the tracked satellites can be calculated by the code observation data, so the sight vector $\boldsymbol{s}^k$ can be obtained. To solve the baseline vector by Eq. (5), the line bias parameter should be estimated at first. The initial line bias parameter and the SD integer ambiguity can be calibrated in advance by using the long-time average-filtering DD solution [25]. Then the real-time line bias delay Δlb_{ij} is obtained after compensation by using the proposed scheme. With the known $\Delta\phi_{ij}^k$, $\boldsymbol{s}^k$,Δlb_{ij} and ΔN_{ij}^n, the baseline vector $\boldsymbol{b}$ can be obtained. By the above analysis, the key of the SD model is to obtain the line bias delay parameter, which can be achieved by a line bias delay monitoring module.

To obtain the attitude angles, firstly, the baseline vector has to be transformed from the Earth-Centered Earth-Fixed (ECEF) frame into the local east, north, up (ENU) coordinate for the attitude determination application:

$$\begin{bmatrix}b_{\mathrm{E}}\\ b_{\mathrm{N}}\\ b_{\mathrm{U}}\end{bmatrix} = \begin{bmatrix}-\sin\Omega & \cos\Omega & 0\\ -\sin\Lambda\cos\Omega & -\sin\Lambda\sin\Omega & \cos\Lambda\\ \cos\Omega\cos\Lambda & \cos\Lambda\sin\Omega & \sin\Lambda\end{bmatrix}\begin{bmatrix}b_{\mathrm{x}}\\ b_{\mathrm{y}}\\ b_{\mathrm{z}}\end{bmatrix} \tag{6}$$

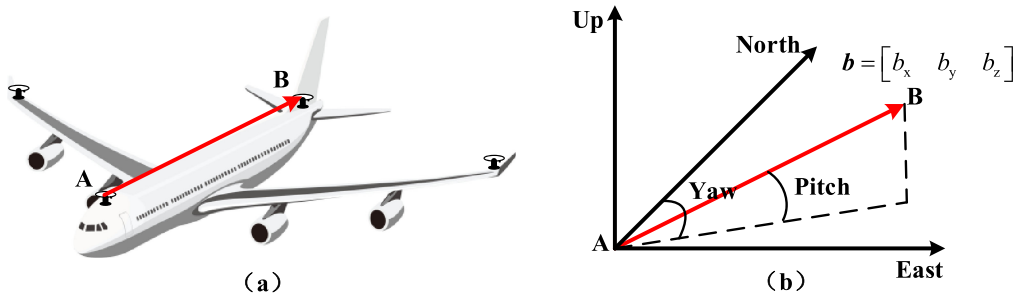

Fig. 1. The relationship between the baseline vector and the attitude angles.

where Λ and Ω are the approximate geodetic latitude and longitude of the vehicle which can be determined by code observations.

As illustrated in Fig. 1, the attitude angles including pitch and heading angles can be deduced by the relationship with the baseline vector in the ENU coordinate:

$$\begin{cases} \tan\alpha = \frac{b_E}{b_N} \\ |b|\sin\beta = b_U \\ |b|\cos\beta = \sqrt{b_E^2 + b_N^2} \\ |b| = \sqrt{b_E^2 + b_N^2 + b_U^2} \end{cases} \tag{7}$$

where α and β are the pitch and heading angles separately.

2.2 The Phase Derived Range Measurement Based Line Bias Delay Monitoring Method

In the SD model, considering that the line biases are the different lengths of signal paths between antennas and the receiver which can be expressed in length as [26]:

$$\Delta lb_{ij} = \frac{2\pi f \Delta L_{ij}}{c}\lambda = 2\pi\Delta L_{ij} \tag{8}$$

To obtain the length difference, conversion of length measurement to phase measurement is effective. Assuming the angle frequency of the sinusoidal signal is $\omega_0 = 2\pi f_0$, the phase shift difference $\Delta\varphi$ of sinusoidal signal after passing through different transmission links can be expressed as:

$$\Delta\varphi(\omega_0) = \omega_0\Delta\tau = \omega_0\frac{\Delta L_{ij}}{c} \tag{9}$$

where $\Delta\tau$ is the time delay difference between the antenna and the receiver. The length difference can be given by:

$$\Delta L_{ij} = \frac{\Delta\varphi(\omega_0)\, c}{\omega_0} \tag{10}$$

The length difference measurement error can be deduced by the equation:

$$\delta\Delta L_{ij} = \frac{\partial\Delta L_{ij}}{\partial\Delta\varphi}\delta\Delta\varphi + \frac{\partial\Delta L_{ij}}{\partial\omega_0}\delta\omega_0 \tag{11}$$

where $\delta\Delta\varphi$ and $\delta\omega_0$ are the phase difference error and the frequency error. By simplifying the Eq. (11), the length difference measurement error can be expressed as:

$$\delta\Delta L_{ij} = \frac{c}{\omega_0}\delta\Delta\varphi - \frac{\Delta L_{ij}}{\omega_0}\delta\omega_0 \tag{12}$$

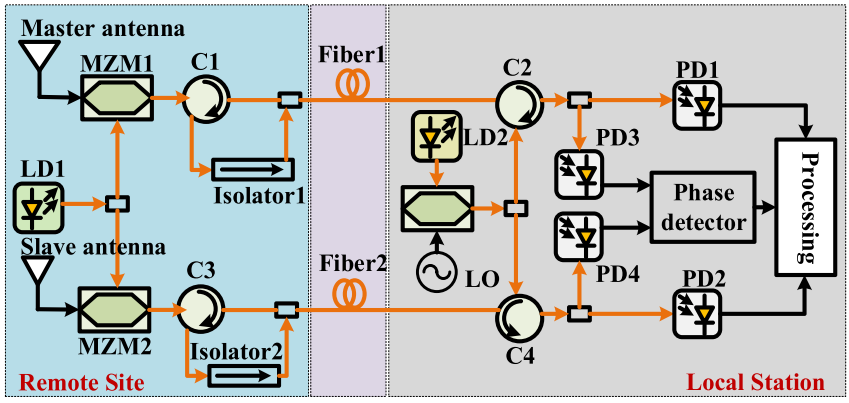

Fig. 2. Schematic diagram of the proposed multi-antenna GPS-over-fiber system. LD: laser diode; MZM: Mach-Zehnder modulator; C: circulator; LO: Local oscillator: PD: photodetector.

From Eq. (12), it can been that the length difference measurement error consists of two parts, one is the fixed error $\delta\Delta\varphi/\omega_0$ which is decided by the error of phase detector, the other is ratio error $\frac{\Delta L_{ij}}{\omega_0}\delta\omega_0$ which is decided by the stability performance of the frequency source and the measurement range.

2.3 The Proposed GPS-Based Attitude Determination System

In a multi-antennae GPS-based attitude determination system, one of the antennas serves as the master antenna, others are slave antennas. The master antenna is used as the reference antenna which is installed at the tail of an aircraft. The slave antenna is installed in the nose. The baseline is defined as the vector from the tail to nose. The direction of the baseline is the attitude of the aircraft. With the pre-defined master antenna, every slave antenna can be used to form a baseline, which can be utilized to calculate two attitude angles.

The scheme of the proposed multi-antenna GPS-based attitude determination system is shown in Fig. 2. The system consists of the remote receiving part, GPS-over-fiber links, the line bias delay monitoring modules and a local signal processing unit. At the remote site, GPS signals are received by the master and slave antennas, then converted into optical signals using a laser diode (LD) and a Mach-Zehnder modulator (MZM). The optical signals are delivered into the local data processing center via an optical fiber. Then the signals are detected by photodetectors (PDs) and processed by a GPS receiver.

At the local station, an optical carrier from another LD is modulated by a sinusoidal signal, which is split into different transmission channels as the delay measurement signal. The delay measurement signal is inserted into the optical fiber through a circulator (C2 or C4) and transmitted to the antennas. With a circulator (C1 or C3), an isolator and an optical coupler (OC) at the remote site, the delay measurement signal is reflected back to the receiver. After passing through the circulators (C2 and C4), delay measurement signals from two paths are converted to electrical signals. In the local station, the phase of two delay measurement signals are compared, which generates the phase difference. The phase difference is proportional to the length difference of two transmission links which can be used to detect the line bias in the GPS measurement system. Then the baseline can be deduced and converted to the attitude angles.

3. Experiment Results and Discussion

A proof-of-concept experiment is carried out based on the scheme shown in Fig. 2. A light wave at 1550 nm is generated from a laser source (TeraXion) with the output power of 15.6 dBm and split to two GPS-over-fiber links by an optical coupler. A lithium niobate intensity modulator (Avanex)

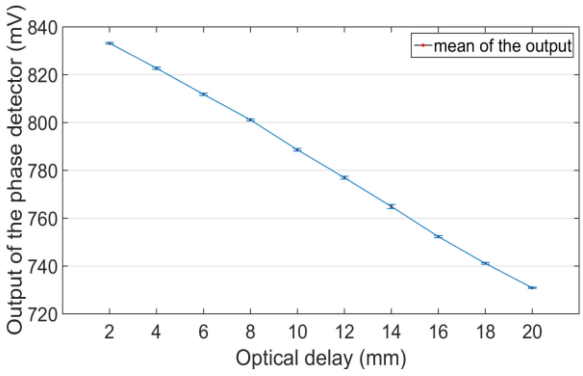

Fig. 3. The output of the phase detector as a function of the optical delay.

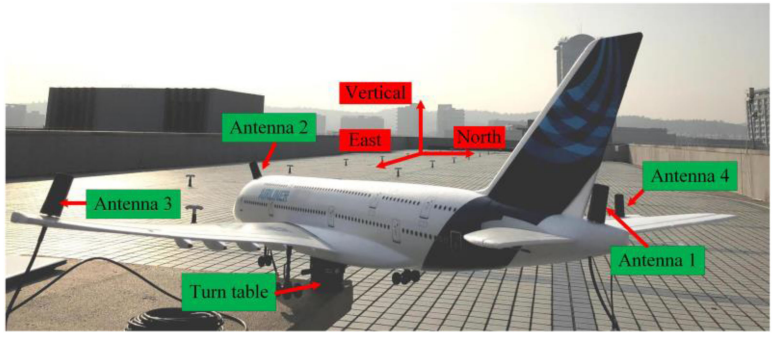

Fig. 4. The experiment setup for the outdoor measurement.

with bandwidth of 13 GHz and a half-wave voltage of 5 V while a PD with bandwidth of 20 GHz, responsivities of 0.61 A/W are used.

3.1 The Performance of the Line Bias Delay Monitoring Module

In the line bias delay monitoring module, a sinusoidal signal with a frequency of 2 GHz is generated and split into two different transmission channels. The phase difference of such two signals is detected by a phase detector (Analog devices AD8302) with measure frequency up to 2.7 GHz and measure power range from −60 dBm to 0 dBm. In our experiment, a variable optical delay line (VODL) is utilized to emulate the variation of the line bias. The output of the phase detector is recorded while the VODL changes 10 times by a step of 2 mm. Fig. 3 shows the relationship between the optical delay and the output of the phase detector. A linear curve with a slope of ∼5.8 mV/mm can be observed clearly. By calculating the standard deviation (STD) of each measurement, the maximum of the STD can be obtained as 0.85589 mV, which means the precision is 0.148 mm.

3.2 The Measurement Precision of the Proposed GPS-Over-Fiber System

Outdoor experiments are carried out to verify the performance of the proposed system. As is shown in Fig. 4, a UAV with a wingspan of 1.52 m and a fuselage of 1.43 m is used as the test object. The test is carried on the roof of a building to track more GPS satellites as well as to avoid the multipath effect. The GPS antennas are rigidly fixed in known positions relative to each other on the UVA. In order to realize three-dimensional attitude measurement, at least two baselines are required. In our experiment, four antennas are used to form two baselines, the front-back baseline consisting of the

Fig. 5. The three-dimensional turn table instrument used as reference rotation angles.

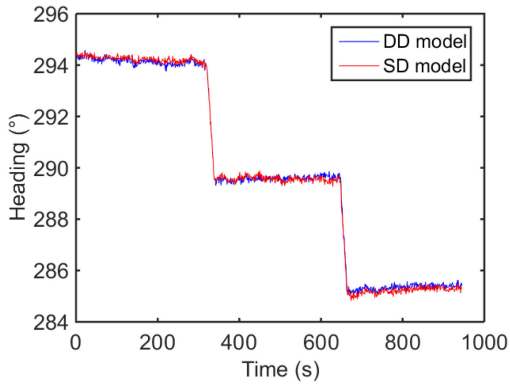

Fig. 6. Heading angle measurement result of the conventional DD model and the SD model.

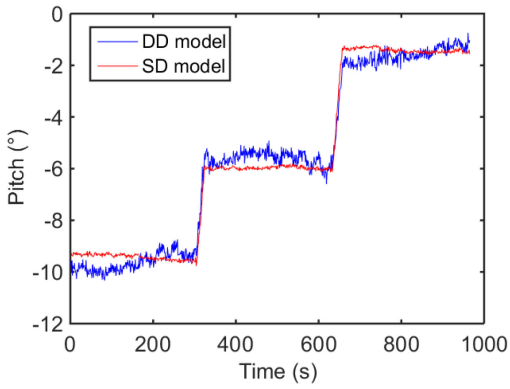

Fig. 7. Pith angle measurement result of the conventional DD model and the SD model.

antenna 1 and 2 is used to calculate the heading and pitch angles, the left-right baseline consisting of antenna 3 and 4 is used to determine the roll angle.

As illustrated in Fig. 5, to emulate the attitude change of a vehicle, a three-dimensional high precision turn table instrument is used as the reference rotation, because it was possible to have its reference rotation angle known at 0.1 degree level. Three cases of experiments are carried out to verify the precision of the three attitude angles.

To change the three-dimensional attitude angles, the turn table instrument is rotated about 5 degrees for two times. The attitude determination results of the conventional DD model and the SD model using the proposed system is shown in Figs. 6–8. The STD and the angle change of the three components of the DD model and the SD model are compared in Table 1, 2 and 3.

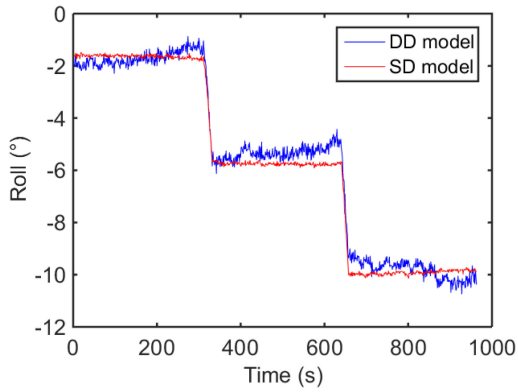

Fig. 8. Roll angle measurement result of the conventional DD model and the SD model.

TABLE 1
Heading Angle Measurement Result by the DD Model and the SD Model Using the Proposed Architecture

Stage	RMS of DD (°)	Mean of DD (°)	RMS of SD (°)	Mean of SD (°)
1	0.1338	294.1525	0.1086	294.2472
2	0.1040	289.5839	0.1067	289.5671
3	0.1102	285.3497	0.1217	285.2181

TABLE 2
Pitch Angle Measurement Result by the DD Model and the SD Model Using the Proposed Architecture

Stage	RMS of DD (°)	Mean of DD (°)	RMS of SD (°)	Mean of SD (°)
1	0.3420	-9.6459	0.1052	-9.4136
2	0.2733	-5.6203	0.0630	-5.9726
3	0.2991	-1.6005	0.0871	-1.4198

The heading angle measurement result is shown in Fig. 6. The measurement results of SD model are very close to those of the DD model. As seen in Table 1, if carefully compared with the results of the DD model, the STD of the SD model decreases in the first stage while increases in the third stages. Due to the tiny difference, the proposed system has little influence on the precision of the heading angle measurement.

Regarding the pitch angel measurement, the SD model still provides a high measurement precision as the heading angel, while that calculated by the DD model significantly reduces. As seen in Table 2, the precision of the pitch angel is improved from 0.3420° by the DD model to 0.1052° by the SD model in stage 1, from 0.2733° by the DD model to 0.0630° by the SD model in stage 2 and from 0.2991° by the DD model to 0.0871° by the SD model in stage 3, indicating an improvement of 3.25 times, 4.34 times and 3.43 times separately. Therefore the proposed system can significantly increase the measurement precision of the pitch angle.

As seen in Fig. 8, the roll angle measurement result is similar with the pitch angle measurement result. As seen in Table 3, the precision of the roll angel is improved from 0.2718° by the DD model to 0.0609° by the SD model in stage 1, from 0.2567° by the DD model to 0.0534° by the SD model

TABLE 3
Roll Angle Measurement Result by the DD Model and the SD Model Using the Proposed Architecture

Stage	RMS of DD (°)	Mean of DD (°)	RMS of SD (°)	Mean of SD (°)
1	0.2718	-1.7099	0.0609	-1.6327
2	0.2567	-5.3195	0.0534	-5.7576
3	0.3531	-9.8241	0.0788	-9.9196

in stage 2 and from 0.3531° by the DD model to 0.0788° by the SD model in stage 3, indicating an improvement of 4.46 times, 4.80 times and 4.48 times separately.

To conclude, the experiment results show that the precision of the pitch angel and the roll angle can be greatly improved by using the proposed method, while the precision of the heading angle is not reduced.

4. Conclusion

A multi-antenna GPS-over-fiber system with a line bias delay monitoring module is proposed and demonstrated for attitude determination. In the proposed system, an external-modulation based analog photonic link is used for long distance transmission of the GPS signals. A carrier phase SD model is also used to eliminate the receiver's clock parameter by using a multi-antenna synchronous GPS receiver to improve the vertical precision. In addition, a photonics-based scheme is applied to compensate for the line bias delay between different GPS channels to meet the condition of carrier phase SD model. Outdoor measurement results of the proposed system based on the conventional DD model and the SD model were compared, and an over 3 times improvement of the vertical positioning precision was achieved which means the vertical precision can reach the same level as the horizontal precision.

References

[1] S. Byeon, S.-H. Mok, H. Woo, and H. Bang, "Sensor-fault tolerant attitude determination using two-stage estimator," *Adv. Space Res.*, vol. 63, no. 11, pp. 3632–3645, 2019.
[2] H. Huang, Z. G. Yang, and J. Zhou, "Microsatellite attitude determination based on skylight polarization and geomagnetic measurement," *Optik*, vol. 178, pp. 1177–1184, 2019.
[3] A. Labibian, S. H. Pourtakdoust, A. Alikhani, and H. Fourati, "Development of a radiation based heat model for satellite attitude determination," *Aerosp. Sci. Technol.*, vol. 82–83, pp. 479–486, 2018.
[4] F. Yu, Z. He, and N. Xu, "Autonomous navigation for GPS using inter-satellite ranging and relative direction measurements," *Acta Astronautica*, vol. 160, pp. 646–655, 2019.
[5] T. P. K. Nguyen, J. Beugin, and J. Marais, "RAMS analysis of GNSS based localisation system for the train control application," in *Proc. Int. Conf. Comput., Manage. Telecommun.*, 2014, pp. 101–106.
[6] K. Wisiol, M. Wieser, and R. Lesjak, "GNSS-based vehicle state determination tailored to cooperative driving and collision avoidance," in *Proc. Eur. Navig. Conf.*, 2016, pp. 1–8.
[7] S. Mansoor, U. I. Bhatti, A. I. Bhatti, and S. M. D. Ali, "Improved attitude determination by compensation of gyroscopic drift by use of accelerometers and magnetometers," *Measurement*, vol. 131, pp. 582–589, 2019.
[8] I. Y. Bar-Itzhack and N. Berman, "Control theoretic approach to inertial navigation systems," *J. Guid., Control, Dyn.*, vol. 11, no. 3, pp. 237–245, 1988.
[9] N. Barbour and G. Schmidt, "Inertial sensor technology trends," *IEEE Sensors J.*, vol. 1, no. 4, pp. 332–339, Dec. 2001.
[10] T. Xu, L. Xu, X. Tian, and X. Li, "GPS-aided method for platform attitude determination based on target images," *Appl. Opt.*, vol. 56, no. 8, pp. 2378–2387, 2017.
[11] A. R. Vetrella, F. Causa, A. Renga, G. Fasano, D. Accardo, and M. Grassi, "Multi-UAV carrier phase differential GPS and vision-based sensing for high accuracy attitude estimation," *J. Intell Robotic Syst.*, vol. 93, no. 1–2, pp. 245–260, 2019.
[12] C. Zhang, L. Ran, and L. Song, "Fast alignment of SINS for marching vehicles based on multi-vectors of velocity aided by GPS and odometer," *Sensors (Basel)*, vol. 18, no. 1, 2018.
[13] S. T. Goh and K. S. Low, "Survey of global-positioning-system-based attitude determination algorithms," *J. Guid. Control Dyn.*, vol. 40, no. 6, pp. 1321–1335, 2017.

[14] R. Santerre, "Impact of GPS satellite sky distribution," *Manuscripta Geodaetica*, vol. 16, no. 1, pp. 28–53, 1991.
[15] G. Lachapelle, M. E. Cannon, and G. Lu, "High-precision GPS navigation with emphasis on carrier-phase ambiguity resolution," *Marine Geodesy*, vol. 15, no. 4, pp. 253–269, 2009.
[16] W. T. Chen, H. L. Qin, Y. Z. Zhang, and T. Jin, "Accuracy assessment of single and double difference models for the single epoch GPS compass," *Adv. Space Res.*, vol. 49, no. 4, pp. 725–738, 2012.
[17] J. M. B. Oliveira, L. M. Pessoa, H. M. Salgado, G. Proudley, D. Charlton, and H. White, "Experimental evaluation of a differential GPS-over-fiber system for aircraft attitude determination," in *Proc. IEEE Avionics, Fiber-Opt. Photon. Technol. Conf.*, 2013, pp. 75–76.
[18] L. M. Pessoa, J. M. B. Oliveira, D. Coelho, J. C. S. Castro, H. M. Salgado, and M. Fames, "Transmission of differential GPS signals over fiber for aircraft attitude determination," in *Proc. IEEE Avionics, Fiber-Opt. Photon. Dig. CD*, 2012, pp. 80–81.
[19] R. Santerre and G. Beutler, "A proposed GPS method with multi-antennae and single receiver," *Bull. Géodésique*, vol. 67, no. 4, pp. 210–223, 1993.
[20] W. T. Chen and X. Q. Li, "Success rate improvement of single epoch integer least-squares estimator for the GNSS attitude/short baseline applications with common clock scheme," *Acta Geodaetica et Geophysica*, vol. 49, no. 3, pp. 295–312, 2014.
[21] J. H. Keong, "GPS/GLONASS Attitude determination with a common clock using a single difference approach," in *Proc. ION-GPS 99*, 1999, pp. 14–17.
[22] C. E. Cohen and B. W. Parkinson, "Integer ambiguity resolution of the Gps carrier for spacecraft attitude determination," *Guid. Control*, vol. 78, pp. 107–118, 1992.
[23] D. Macias-Valadez, R. Santerre, S. Larochelle, and R. Landry, "Improving vertical GPS precision with a GPS-over-fiber architecture and real-time relative delay calibration," *GPS Solutions*, vol. 16, no. 4, pp. 449–462, 2012.
[24] X. Jiang, X. C. Wang, and S. L. Pan, "A Multi-antenna GNSS-over-fiber system with high vertical precision," in *Proc. Int. Topical Meeting Microw. Photon.*, Toulouse, France, 2018, pp. 1–4.
[25] L. Zhang, Y. Q. Hou, and J. Wu, "A drift line bias estimator: ARMA-based filter or calibration method, and its application in BDS/GPS-based attitude determination," *J. Geodesy*, vol. 90, no. 12, pp. 1331–1343, 2016.
[26] Y. Li, K. Zhang, C. Roberts, and M. Murata, "On-the-fly GPS-based attitude determination using single- and double-differenced carrier phase measurements," *GPS Solutions*, vol. 8, no. 2, pp. 93–102, 2004.